

FEDSM-ICNMM2010-3086 (

S-shaped Pin-fins for enhancement of overall performance of the Pin-fin heat sink

T. J. John

College of Engineering and Science
Louisiana Tech University,
Ruston, LA USA 71272

B. Mathew

College of Engineering and Science
Louisiana Tech University,
Ruston, LA USA 71272

H. Hegab

College of Engineering and Science
Louisiana Tech University,
Ruston, LA USA 71272

ABSTRACT

In this paper the authors are studying the effect of introducing S-shaped pin-fin structures in a micro pin-fin heat sink to enhance the overall thermal performance of the heat sinks. For the purpose of evaluating the overall thermal performance of the heat sink a figure of merit (FOM) term comprising both thermal resistance and pumping power is introduced in this paper. An optimization study of the overall performance based on the pitch distance of the pin-fin structures both in the axial and the transverse direction, and based on the curvature at the ends of S-shape fins is also carried out in this paper. The value of the Reynolds number of liquid flow at the entrance of the heat sink is kept constant for the optimization purpose and the study is carried out over a range of Reynolds number from 50 to 500. All the optimization processes are carried out using computational fluid dynamics software CoventorWARE™. The models generated for the study consists of two sections, the substrate (silicon) and the fluid (water at 278K). The pin fins are 150 micrometers tall and the total structure is 500 micrometer thick and a uniform heat flux of 500KW is applied to the base of the model. The non dimensional thermal resistance and nondimensional pumping power calculated from the results is used in determining the FOM term. The study proved the superiority of the S-shaped pin-fin heat sinks over the conventional pin-fin heat sinks in terms of both FOM and flow distribution. S-shaped pin-fins with pointed tips provided the best performance compared to pin-fins with straight and circular tips.

KEYWORDS

Micro channel heat sinks, Heat sinks, Pin fin, S-shaped pins, Pin-fin heat sinks.

NOMENCLATURE

C_p : specific heat (J/KgK)

H : Height of the model (m)
k : thermal conductivity (W/Km)
L : length of the model (m)
PP : pumping power (W)
 ΔP : pressure drop (kPa)
 q'' : heat flux (W/m²)
R : Thermal resistance (K/W)
T : Temperature (K)
W : width of the model (m)

Subscripts

f : fluid
s : solid
non : non dimensionalized quantity

INTRODUCTION

Need for dissipating heat from micro devices and electronic chips has increased drastically in the last decade, especially with the miniaturization of the devices [1]. Similar to all other micro technologies developed till now, the heat dissipating methods for the micro scale devices are also adapted from the already well developed macro scale technologies. Heat sinks are devices that are used to dissipate heat from any heat generating component and thereby increasing its life time and performance. The applications of heat sinks can be classified into 1) improving the thermal control of electronic devices, assemblies, and other components by increasing the heat dissipation surface area of the device, and 2) increasing the reliability and functional performances of electronic, communication and power systems [1]. Several types of heat sinks which use both air and fluids as the cooling agent have been proposed by researchers in macro scale, and pin-fin heat sink is one of the most promising one among them. The pin-fin heat sinks are preferred over other micro heat sinks due its high heat transfer coefficient [1-7]. In the pin-fin heat sinks the fluid

flow will be continuously disturbed by the fin structures, thereby forming a continuously developing flow which increases the heat transfer efficiency of the heat sink. Recent research has developed several micro pin fin heat sinks with different pin shapes, and some of these shapes have proved to have superior performance over the conventional pin-fin shapes [4.5].

While developing a pin-fin heat sink for micro scale application, the two major design constraints that have to be accounted for are the thermal resistance and pressure drop. By properly optimizing the shape and size of the pin-fin structures inside the heat sink an optimal heat sink can be designed. Another major issue faced during the design phase of the micro pin-fin heat sinks is the formation of the hot spots on the micro pin-fin heat sink where the fluid flow is minimal. This phenomenon will lead to an increase in the temperature at some particular spots on the electronic chip which leads to performance failure. This problem can be solved by using smoothly shaped pin-fin structures and making sure that the thermal resistance of the heat sink is still maintained within an acceptable range. This paper investigates the feasibility of using S-shaped pin-fin heat sinks, which allows a better distribution of the fluid flow inside the heat sink while generating enough disturbances in the flow pattern, thereby keeping the thermal resistance low as possible. The major advantage of using the S-shaped pin-fin structures over other shapes is the better distribution of the fluid flow over the entire heat sink surface, thus avoiding the formation of the hot spots on the heat sink surface. For example, while using the circular pin-fin structures there are certain areas on the heat sink which have almost zero liquid flow; thus forming a hot spot on the surface of the heat sink and resulting in the failure of the electronic chip.

The feasibility and optimization study on the S-shaped heat sink is carried out using computer simulations generated using COVENTORWARE™. The heat sink under consideration in this study has a length and width of 1 cm each and has two layers. Only a small section of the total micro heat-sink is modeled for the purpose of analysis to consider for the memory constraints of the computers and for the ease of analysis. The model consists of two sections, the substrate and the fluid. The substrate used in the bottom layer had a total depth of 500 micrometers, width of 200 micrometers, and length of 1 cm. The pin fins are 150 micrometers tall and the cross sectional width is 10 micrometers. The total width over which the S-shaped pin-fin spreads itself is kept constant at 50 micrometers. Heat sinks with circular pin-fin structures of the same dimensions (radius = 25 μ m) are also developed for the comparison study of the overall performance. An optimization study of the new S-shaped pin-fin heat sink based on the variation of the pitch distance in both axial and transverse direction is also carried out in this paper. The shape of the S-shaped pin-fin structures towards its tip is varied to study its effect on both the pressure drop and thermal resistance of the heat sink.

Silicon is used as the substrate, and uniform heat flux of 500kW/m² is applied at the bottom of the structure. Simulations are carried out for Reynolds numbers at inlet section ranging from 50 to 500. Water with initial temperature of 278.15K was used as the coolant in the heat-sink. After obtaining the numerical results from the models, the nondimensional overall thermal resistance and nondimensional pumping power were calculated from the results. A heat sink of same dimensions without pin-fin structures is developed for the purpose of nondimensionalizing thermal resistance and pumping power obtained from the different models. A figure of merit (FOM) was developed using the nondimensional thermal resistance and nondimensional pumping power for each structure with different pin-fin shapes.

RELEVANT LITERATURES

Park et al. developed a numerical model for the optimization of the Pin-fin heat sink. The objective of optimization was the minimization of the thermal resistance and pressure drop in 2004 [2]. The study was based on Pin-fins with rectangular shapes and the study concluded that both the height and width of the fins are affecting the thermal resistance as well as the pressure drop in the heat sink.

K. Park et al studied the effect of Pin-fin shapes on the thermal resistance and the pressure drop inside a Pin-fin heat sink with the use of computational fluid dynamics [3]. Two shapes of pins, circle and rectangle were considered in the study and the study concluded that the rectangular Pin-fins outperformed the circular fins in the performance of the thermal resistance.

Yavo Pleles et al. conducted a study on the optimization of the micro Pin-fin heat sink with silicon as the substrate and water as the cooling agent [4]. The study showed that the use of micro Pin-fin will decrease the pin efficiency of the heat sink and the paper suggested a solution for the issue by using Pin-fins of smaller height. The study also suggested the usage of low density Pin-fins for a low Reynolds number (liquid flow) application and higher density Pin-fins for higher Reynolds number application. The same group came up with another paper in 2007 studying the thermal resistance and the pressure drop of a micro Pin-fin heat sink [5]. Four different shapes of Pin-fin structures (circle, hydrofoil, cone, and rectangle) were subjected to the analysis. Silicon was used as the substrate and water was used as the cooling agent in this study also.

An optimization based on the entropy generation by five different Pin-fin shapes (Elliptical, rhombus, circle, rectangle and square) inside a heat sink was conducted in 2006 by Abdel-Rehim [6]. Circular and elliptical pins were showing the best thermal performance and copper was found to be the best material for heat sink manufacturing.

T. J. John et al. conducted investigation on the effect of the micro Pin-fin geometries on the performance evaluation of the micro Pin-fin heat sinks in 2009 [7]. Six different geometries were studied under two different conditions, constant liquid flow rate and constant pressure drop. Geometries selected for the study were square, circle, rectangle, ellipse, triangle and

rhombus. The substrate material used was silicon and a figure of merit (FOM) term was developed as an evaluation criterion for the micro heat sink. The study reported that at very low flow rate the thermal resistance factor is the dominating term in determining FOM and ellipse was the best performer among the all structures. At intermediate flow rates the circular pin had the best performance and as the flow rate increased the pumping pressure became the dominating factor in FOM and the rectangle pin-fin dominated the evaluation.

Qu w. and Mudawar I. studied the three dimensional fluid flow and heat transfer inside a micro channel heat sink numerically, and the solutions were obtained using simple algorithm [8]. Even though the study didn't reveal any exiting results the work provided a detailed discussion on the numerical analysis of the fluid flow and heat transfer and provided a good understanding on the validation of the numerical analysis.

THEORY

A top view of the micro pin fin heat sink along the Z- and the X- axis are shown in Fig. 1. The total length of the micro pin fin heat sink along the X-axis is L, the width W, and the total height H. While solving the numerical equations for this model, certain assumptions were made.

1. The microfluidic device under consideration is operating under steady state.
2. The fluid does not undergo phase change while flowing through the microfluidic device.
3. Non slip boundary condition is assigned to the walls in contact with the fluid in the model.
4. The fluid is assumed to be incompressible.
5. The thermo physical properties are assumed constant.
6. Phenomenon such as viscous heat dissipation and flow maldistribution are considered negligible.

The temperature profile, pressure drop and the flow pattern in the repeating unit of the micro pin-fin heat sink is obtained by solving four governing equations numerically using CoventorWare™. These governing equations consist of continuity equation, three momentum equations and two energy equations. The above mentioned governing equations in vector form can be represented as follows:

$$\nabla \cdot \vec{V} = 0 \quad (1)$$

$$\rho(\vec{V} \cdot \nabla \vec{V}) = -\nabla P + \mu \nabla^2 \vec{V} \quad (2)$$

$$\rho \vec{V} C_p \nabla \cdot T_F = k_F \nabla^2 T_F \quad (3)$$

$$k_S \nabla^2 T_S = 0 \quad (4)$$

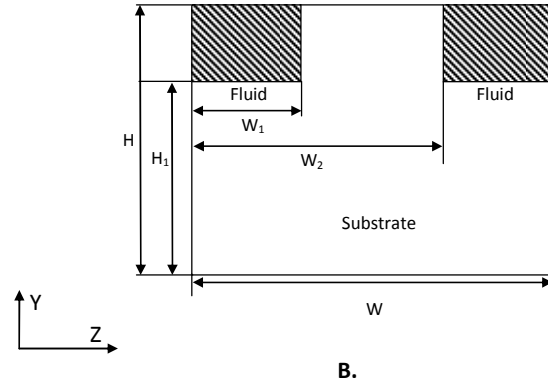
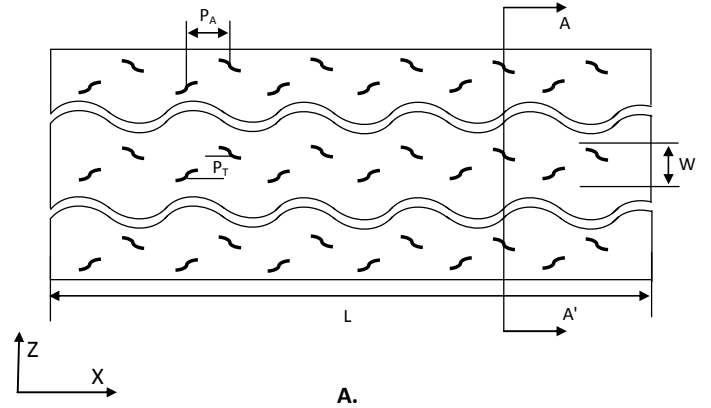


Figure 1: Top view and cross sectional view of the pin-fin heat sink A) along x axis B) along z axis

Equation 1 is the continuity equation and Eq. 2 represents the momentum equation of the repeating unit. Equations 3 and 4 are the energy equations for the liquid and silicon substrate respectively. Certain boundary conditions are to be defined in order to solve the governing equations of the current model and these are discussed below. The liquid velocity at the inlet section of the micro pin-fin heat sink in the X-direction (V_x) is an input parameter for this model. It is calculated from the liquid flow rate (Eq. 5) and the cross sectional area of the repeating unit by assuming uniform flow rate at the inlet section of the repeating unit. The velocities in the other two directions at the inlet section are taken to be zero. The pressure at the outlet of the device is assumed to be zero. For the actual liquid flow through the heat sink the pressure at the outlet of the heat sink need not always be zero. However, in this study, as the pressure drop across the heat sink is the only point of interest the assumption is valid and is given by Eq. 6. One of the assumptions made towards the beginning of this study is that the liquid velocity at the walls of the channel is zero and is represented using Eq. 7.

$$\dot{V}_{in} = \dot{v} \quad (5)$$

$$P_{out} = 0 \quad (6)$$

$$\vec{V}_{wall} = 0 \quad (7)$$

Equations 8 and 9 represent the boundary conditions used for solving the energy equation of the substrate. In order to simulate the actual heat transfer scenario in a heat sink, a uniform heat flux is applied at the bottom of the model and is represented using Eq. 8. In case of an actual heat sink made on the silicon wafer, the top surface will be bonded to a glass plate. Thus, heat transfer (heat loss) through the top of the pin-fin structure is negligible in comparison with heat transfer through other surfaces. Accordingly, for the easiness of simulation the top of every pin-fin is considered to be insulated as represented by Eq. 9 ($\partial\Omega_T$ represents the top surface of the pin-fins).

$$-k_s \frac{\partial T_s}{\partial y} \Big|_{x,y=0,z} = q'' \quad (8)$$

$$\frac{\partial T_s}{\partial y} \Big|_{\partial\Omega_T} = 0 \quad (9)$$

As the model considered in the study is only a small section of a micro pin-fin heat sink, both sides of the substrate are assigned symmetry boundary conditions. This assumption is made based on the fact that the repeating unit modeled in the study can be replicated towards both sides forming the full heat sink. In addition, the inlet and outlet sections of the substrate are also considered to be insulated from heat loss to the surroundings which can either be the ambient or the bulk substrate (Eq. 10).

$$\frac{\partial T_s}{\partial x} \Big|_{x=L,y,z} = \frac{\partial T_s}{\partial x} \Big|_{x=0,y,z} = 0 \quad (10)$$

$$\frac{\partial T_s}{\partial z} \Big|_{x,0 \leq y \leq H, z=0} = \frac{\partial T_s}{\partial z} \Big|_{x,0 \leq y \leq H, z=W} = 0 \quad (11)$$

Equations 12 to 16 represent the boundary condition used for solving the energy equation of the liquid. The liquid at the inlet section is kept at a constant temperature of 278.15 K and the outlet section of the liquid is considered to be adiabatic, i.e. heat transfer through the outlet section of the liquid is zero. Equations 12 and 13 represent these two conditions.

$$T_F \Big|_{x=0,y,z} = T_{in} \quad (12)$$

$$\frac{\partial T_F}{\partial x} \Big|_{x=L,y,z} = 0 \quad (13)$$

As discussed earlier in the case of the substrate, both sides of the liquid are considered to be symmetric. Thus, the heat transfer and fluid flow through these walls is set at zero (Eq. 14 and Eq.15). The heat loss from the top of the liquid to the ambient is considered to be zero, same as in the case of pin-fin top surface explained earlier in this study. This condition is obtained using the boundary condition given by Eq. 16. The heat transfer from the substrate to the liquid through the interface between the two is defined using Eq. 17. Here $\partial\Omega$ represents the interface between the solid and liquid.

$$\frac{\partial T_F}{\partial z} \Big|_{x,H \leq y \leq H, z=0} = \frac{\partial T_F}{\partial z} \Big|_{x,H \leq y \leq H, z=W} = 0 \quad (14)$$

$$\frac{\partial P}{\partial z} \Big|_{x,H \leq y \leq H, z=0} = \frac{\partial P}{\partial z} \Big|_{x,H \leq y \leq H, z=W} = 0 \quad (15)$$

$$\frac{\partial T_F}{\partial y} \Big|_{x,y=H, 0 \leq z \leq W} = \frac{\partial T_F}{\partial y} \Big|_{x,y=H, W \leq z \leq W} = 0 \quad (16)$$

$$k_F \frac{\partial T_F}{\partial \vec{n}} \Big|_{\partial\Omega} = k_S \frac{\partial T_S}{\partial \vec{n}} \Big|_{\partial\Omega} \quad (17)$$

All the above governing equations subjected to the above boundary conditions are solved using CoventorWare™. It employs a finite volume method to solve all the governing equations using the appropriate boundary conditions. The second order upwind scheme is used for discretizing the convective terms and the central different scheme is used for the diffusive terms of these equations. In the case of the models with micro channels as the second layer the boundary condition at $z=0$ and W and $y=H$ will change accordingly.

In this study, both the thermal resistance as well as the pumping power is used for achieving the optimal structure design. The thermal resistance is calculated as the ratio of the difference between the maximum temperature of the substrate and the inlet temperature of the liquid to the heat applied at the bottom of the substrate (Eq. 18). Pumping power across the channel needed for the analysis is calculated as the product of pressure drop and flow rate of the liquid (Eq. 19).

$$R_{th} = \frac{T_{S,out} - T_{F,in}}{q} \quad (18)$$

$$PP = \Delta P \times \dot{V} \quad (19)$$

The pumping power and the thermal resistance attained at each flow rate and pressure drop of different structures are nondimensionalized using the thermal resistance and pumping power obtained from a model of the same overall dimensions

but without any pin-fin structures in it as shown in Eq. 20 and 21.

$$R_{th,non} = \frac{R_{th,stu}}{R_{th,without_stu}} \quad (20)$$

$$PP_{non} = \frac{PP_{stu}}{PP_{without_stu}} \quad (21)$$

Since the optimization of the pin-fin shape is a multi objective problem, a weighted average method is used for calculating the FOM in this analysis [2]. The FOM is calculated as follows.

$$FOM = \frac{1}{(n_1 \times R_{th,non}) \times (n_2 \times PP_{non})} \quad (22)$$

Where $n_1 + n_2 = 1$

By varying the values of n_1 and n_2 the relative contribution of each parameter in FOM can be determined according to the objective of the design. In normal situations, the value of n_1 and n_2 is taken as 0.5, thus giving equal significance to each function used for determining FOM. As the pumping power and the thermal resistance are inversely proportional to FOM; the higher the FOM, the better the overall performance of the heat sink. The maximum, minimum, and average temperature at the outlet of both the substrate and the liquid is measured along with the pressure drop and flow rate across the channel for further analysis.

MESH DEPENDENCY AND OPTIMIZATION

In order to obtain an accurate solution of the governing equations solved numerically using CoventorWare™ an appropriate meshing scheme has to be used with every model. For the study presented in this paper extruded meshing schemes is used to obtain the accurate solution of the governing equations. In the extruded meshing scheme the top X-Y plane of the model is meshed initially using the specified mesh setting and then the generated surface mesh is extruded in the Z-direction. Element size in the extruding direction is also a user defined quantity in CoventorWare™. Two different strategies are used to reach the optimized mesh setting for each of the models considered in this study. In the first strategy, the mesh sizes are varied till the maximum difference in liquid flow rate between the inlet and outlet section of the repeating unit is less than 0.1%. This strategy is used since mass flow rate has to be conserved across every face normal to flow for a heat sink. The second strategy used to obtain the optimized mesh setting is by checking the grid dependency of the meshed models. In this strategy the mesh dimensions are refined continuously and the output parameters like maximum substrate temperature, flow rate and pressure drop of the device are compared with the results obtained from the previously refined mesh model. If the maximum relative change in these parameters in comparison

with from the previously refined mesh is within an acceptable range (less than 0.5%) the mesh is considered to be optimized. The maximum and minimum element size for the extruded meshing scheme along the XY plane is 25μm and 15μm and along Z direction is 12μm and 8μm.

RESULTS

In order to study the superiority of the S-shape pin-fin heat sink based on both FOM and flow distribution, a model with circular pin-fin structures of same radius was developed in the study. The results obtained for the thermal resistance, pressure drop and the FOM term are shown in figures 2a through 2c.

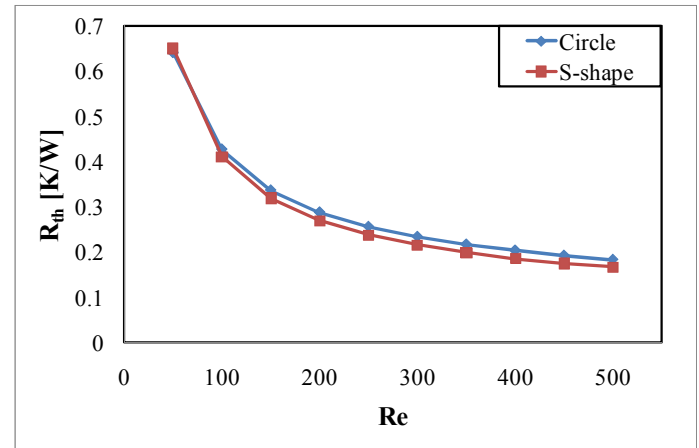


Figure 2a: Variation in thermal resistance for circular and S-shaped pin-fin structures for various values of Re.

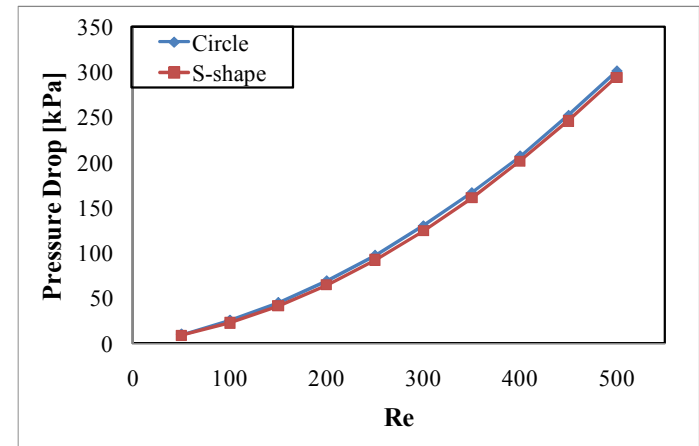


Figure 2b: Variation in pressure drop for circular and S-shaped pin-fin structures for various values of Re.

From figure 2b, it can be noted that the magnitude of pressure drop while using both pin-fin shapes remains close to one another. The overall thermal resistance of the heat sink with S-shaped pin-fin structure is lower than the heat sink with circular pin-fin. And this variation is more predominant at higher values of Reynolds numbers. The reduction in the thermal resistance while using the S-shaped pin-fin structures

leads to the increase in the FOM term. This can be observed from figure 2c. In this comparison study, S-shaped pin-fin structures with straight edges are used. Later in this section, the variation in the FOM with different shapes of S-shaped pin-fin structures are studied, and it can be observed that the FOM is much higher for S-shaped pin-fins with pointed edges.

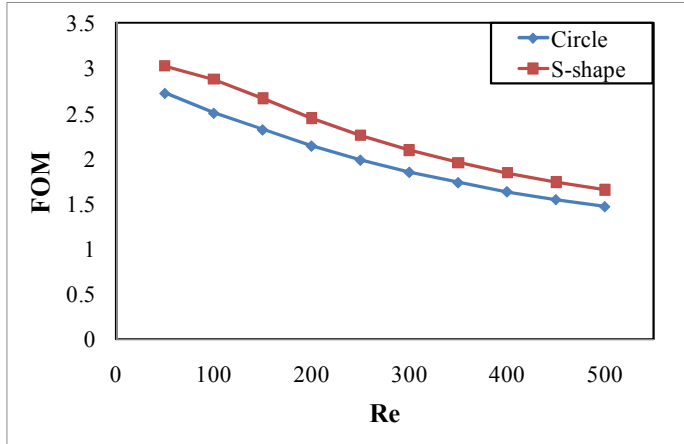


Figure 2c: Variation in FOM for circular and S-shaped pin-fin structures for various values of Re.

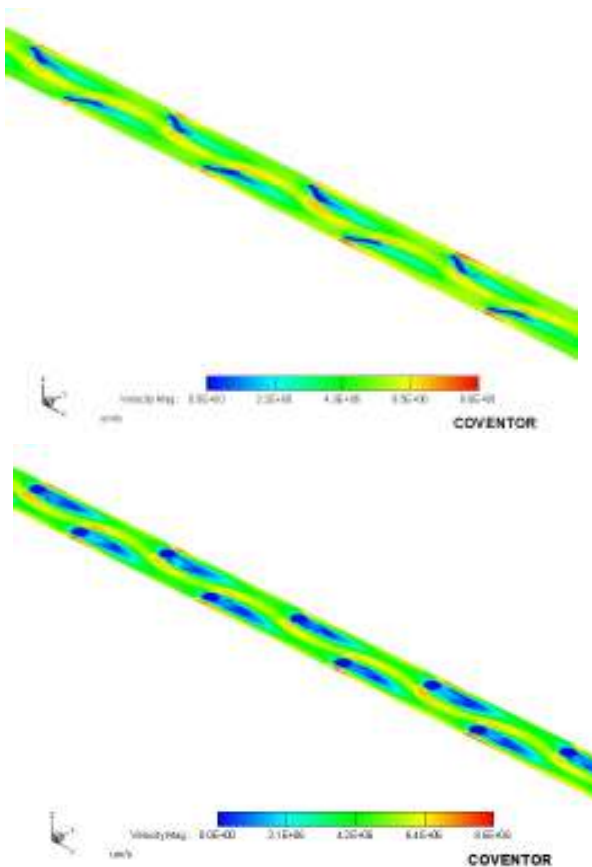


Figure 3: Contour plot showing the flow distribution inside the heat sinks with both S-shaped and circular pin-fins.

Though the pressure drop remains the same, reduction in the thermal resistance can be explained by looking at the flow pattern in both heat sinks and is given in figure 3. From figure 3, it can be seen that at a Reynolds numbers of 400 the flow distribution inside the heat sink with S-shaped pins are much evenly distributed than in the one with circular pin-fins. In the heat sink with circular pin-fins certain areas behind the circular pin-fins have almost zero fluid velocity, which causes the generation of hot spots. But as seen from the contour plot the heat sink with S-shaped pin-fins have fluid flow all over the heat sink eliminating the chance of hot spot generation.

The overall performance optimization of the heat sinks with S-shaped pin-fins based on variation in pin-fin tip shapes is studied in this section. The initial pin-fin structures subjected to study were having straight tip, and in this section S-shaped pin-fins with pointed and circular tips were also subjected to study and compared with each other. Figure 4 shows the three different tip shapes of the S-shape pin-fin structures.

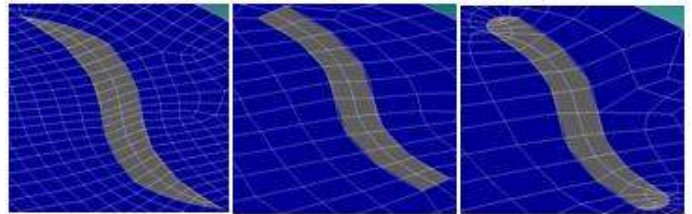


Figure 4: Different tip shaped of S-shaped pin-fin structure used for the optimization purpose.

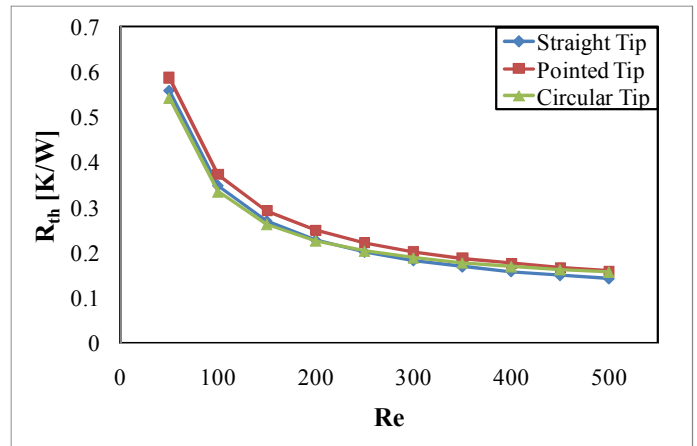


Figure 5a : Variation in thermal resistance for S-shaped pin-fin with different tip shapes for various values of Re.

Figures 5a through 5c show the thermal resistance, pressure drop and the FOM for the tip shape optimization study. Figure 5a represents the comparison between the thermal resistances obtained along the heat sink for three different tip shapes for various Reynolds numbers. It can be observed that the S-shaped pin-fin with the pointed tip is having the highest thermal resistance and the one with the straight tips is having the lowest thermal resistance. The pins with circular and straight tips have their thermal resistance very close to each

other. This is due to the higher disturbance of the fluid flow generated by the pin-fin structures having the straight tips compared to the others. The pressure drop plot given in figure 5b shows that the pin-fin structures having the pointed tips is having the least pressure drop and the one with straight tip is having the highest pressure drop. Even though pins with the pointed tips are having the highest thermal resistance, it has the highest value for the FOM term due to the least pressure drop attained across it. So when equal weight is given to the thermal resistance and pressure drop while calculating the FOM term, the pointed tipped pin-fin structures shows better overall performance. Figure 5c gives the plot of the FOM for all the three heat sinks with three different tip shapes.

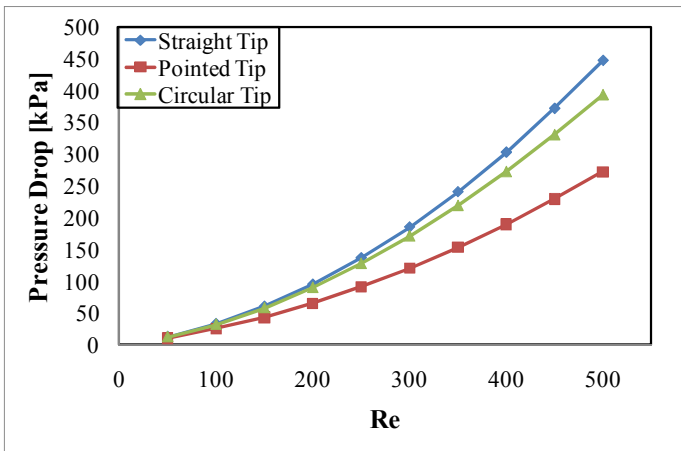


Figure 5b: Variation in pressure drop for S-shaped pin-fin with different tip shapes for various values of Re.

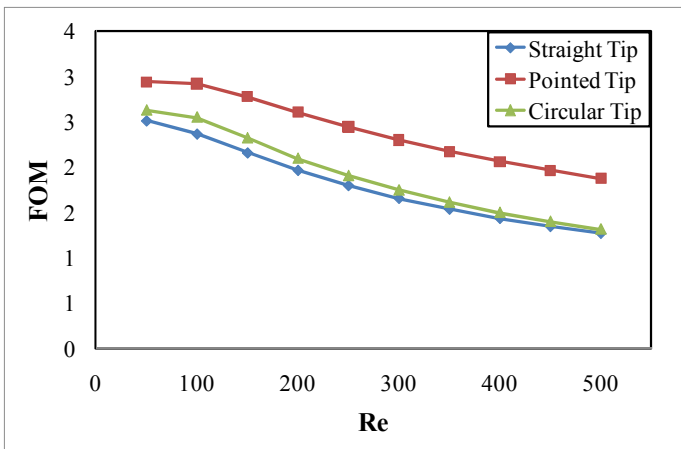


Figure 5c: FOM for S-shaped pin-fin with different tip shapes for various values of Re.

It can be also noted from figure 5c that the FOM for circular and straight tip shaped pin-fin structures stays close to each other at high values of Reynolds numbers and shows little variation for low values of Reynolds numbers. At low values of Reynolds number, the thermal resistance is an important

contributor towards the FOM term but loses its dominance as the magnitude of the Reynolds number increases.

The effect of the overall performance of the pin-fin heat sinks with S-shaped structures based on the variation of the pitch distance is studied in this section. The distance from the center of a pin-fin structure towards the center of the adjacent pin-fin is taken as the pitch distance. The pitch distance in the transverse direction is considered first in this study. The pitch distance in the transverse direction is varied as 25 μ m, 50 μ m and 75 μ m. The thermal resistance and the pressure drop along the heat sink with the different transverse pitch distances are plotted in the figures 6a and 6b.

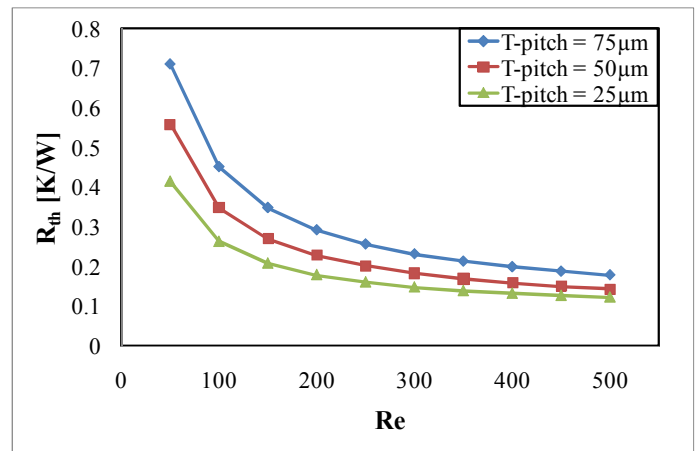


Figure 6a : Variation in thermal resistance for S-shaped pin-fins for different transverse pitch distance with various values of Re.

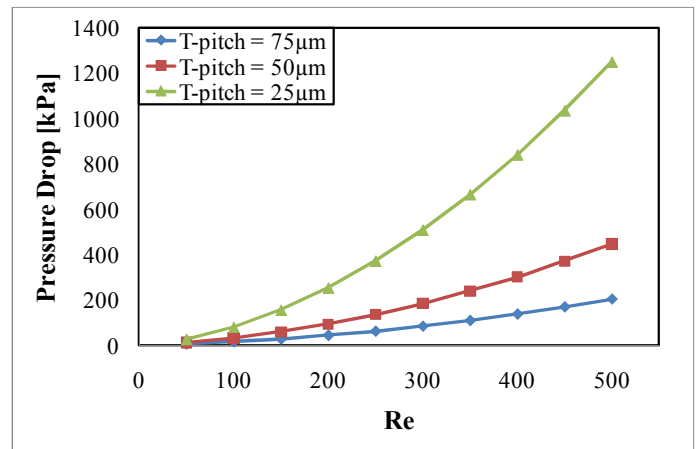


Figure 6b : Variation in pressure drop for S-shaped pin-fins for three different transverse pitch distance.

The plot shows a clear variation in the thermal resistance with increase in the transverse pitch distance. The pitch distance in the transverse direction is inversely proportional to the thermal resistance. As the pitch distance is increased the number of pin-fin structures available to disturb the fluid flow

decreases, thus increasing the thermal resistance across the heat sink. Figure 6b shows the plot of pressure drop across the heat sinks for the values of transverse pitch. The variation in the pressure drop across the heat sink is very dominant in the case study. It can be observed from figure 6b that as the transverse pitch distance is reduced from $75\mu\text{m}$ to $50\mu\text{m}$ the variation in pressure drop is quite high, but as the distance is reduced to $25\mu\text{m}$ the variation in the pressure drop attains a huge shift. This variation in the pressure drop value dominates the FOM term. The FOM variation for all three values of the transverse pitch distance is represented in figure 6c. The FOM of the heat sink with maximum transverse pitch distance is the best due to the lowest pressure drop across it.

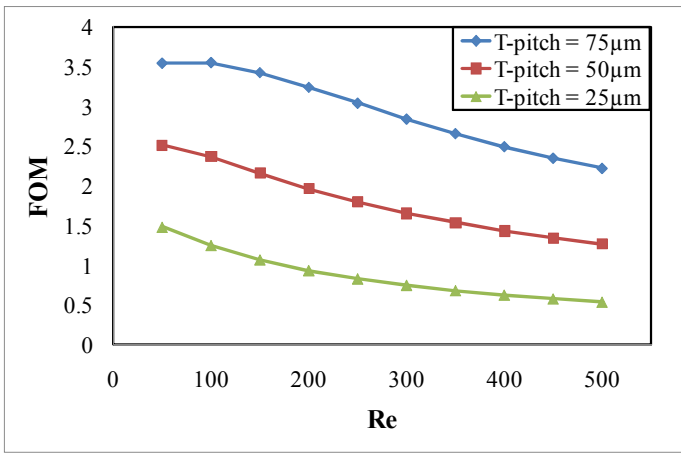


Figure 6c: Variation in FOM for S-shaped pin-fins for three different transverse pitch distance with various values of Re.

The variation in the overall performance of the pin-fin heat sink with the variation in the axial pitch distance is discussed in this section. The study is conducted for three values of axial pitch distance: $100\mu\text{m}$, $200\mu\text{m}$ and $300\mu\text{m}$.

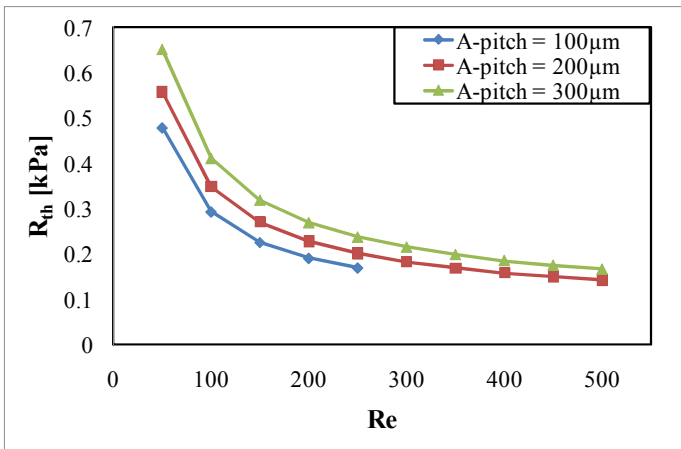


Figure 7a : Variation in thermal resistance for S-shaped pin-fins for different axial pitch distance with various values of Re.

The numerical study on model with pitch distance of $100\mu\text{m}$ is limited to a Reynolds number of 250 due to the difficulty in attaining the convergence criteria due to the high pressure drop formed across it for higher values of Reynolds numbers. The study involving the variation in the axial pitch distance also follows the same trend as of the results from the study involving transverse pitch distance. As the pitch distance is increased the thermal resistance increases and the pressure drop decreases (Figure 7b).

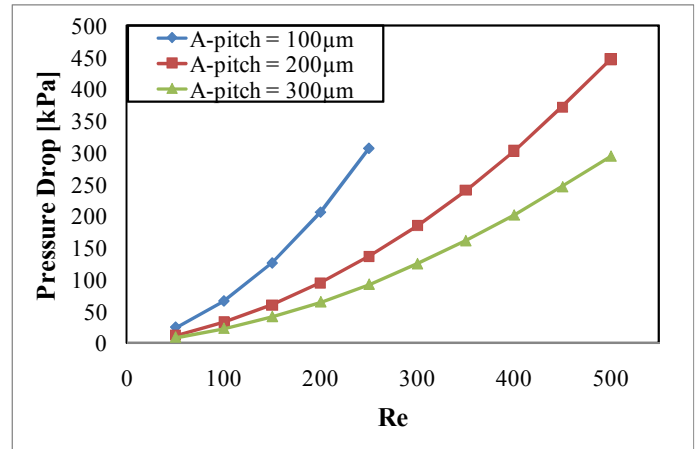


Figure 7b : Variation in pressure drop for S-shaped pin-fins for three different axial pitch distance with various values of Re.

With the increase in pressure drop it will again dominate the FOM calculation and is plotted in figure 7c. The FOM for the model with highest axial pitch shows the best results and the model with shortest pitch distance show the worse performance.

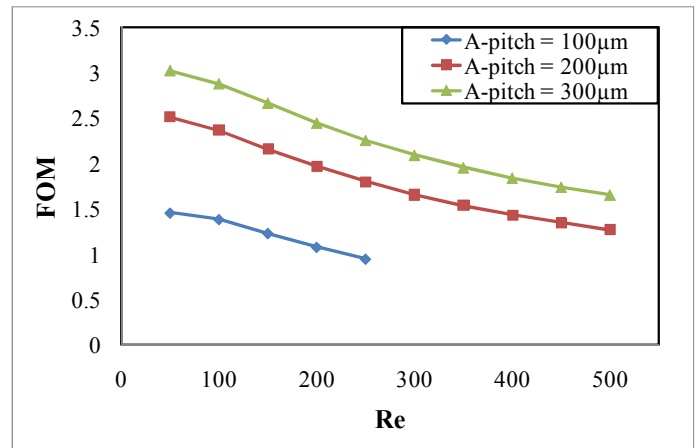


Figure 7c : Variation in FOM for S-shaped pin-fins for three different axial pitch distance with various values of Re.

From the optimization study based on the pitch distance in both axial and the transverse direction it can be noted that the pressure drop is the major contributor in the FOM calculation.

This leads to the conclusion that while determining an optimal pitch distance for the micro pin fin heat sink, the maximum acceptable pressure drop has to be determined first and based on the value of the selected pressure drop, the FOM term can be used to determine the optimal pitch distance in both directions.

CONCLUSION

The feasibility of using S-shaped Pin-fin structures in heat sink is numerically investigated using CoventorWare™ in this paper. An optimization based on the pitch distance in both axial and transverse directions is studied, and the effect of the pin-fin tip shape is investigated in the study. The major conclusions of the investigation are as follows.

1. The S-shaped pin-fin structures show better overall performance compared to the conventional pin-fin structures like circles, in terms of both FOM and fluid flow distribution.
2. S-shaped pin-fin heat sinks have the advantage of avoiding the hot spots which can cause the failure of the electronic chips.
3. S-shaped pin-fins with pointed edges show the best performance compared to the S-shaped pins with straight and circular tips.
4. Pressure drop is the major factor in the FOM calculation while trying to optimize the pin-fin pitch distances in both directions.

REFERENCES

- [1] H.-T. Chen, P.-L. Chen, J.-T. Horng, Y.-H. Hung, "Design optimization for pin-fin heat sinks," *Journal of Electronic Packaging, Transactions of the ASME*, vol. 127, no. 4, pp. 397-406, 2005.
- [2] K. Park, D.-H. Choi, K.-S. Lee, "Numerical shape optimization for high performance of a heat sink with pin-fins," *Numerical Heat Transfer; Part A: Applications*, Vol. 46, No. 9, pp. 909-927, 2004.
- [3] K. Park, K.-H. Rew, J.-T. Kwon, B.-S. Kim, "Optimal solutions of pin-fin type heat sinks for different fin shapes," *Journal of Enhanced Heat Transfer*, Vol. 14, No. 2, pp. 93-104, 2007.
- [4] A. Kosar, Y. Peles, "TCPT-2006-096.R2: Micro scale pin fin heat sinks - Parametric performance evaluation study," *IEEE Transactions on Components and Packaging Technologies*, Vol. 30, No. 4, pp. 855-865, 2007.
- [5] Y. Peles, A. Kosar, C. Mishra, C.-J. Kuo, B. Schneidern, "Forced convective heat transfer across a pin fin micro heat sink," *Journal of Electronic Packaging, Transactions of the ASME International Journal of Heat and Mass Transfer*, Vol. 48, No. 17, pp. 3615-3627, 2005.
- [6] Z. S. Abdel-Rehim, "Optimization and thermal performance assessment of pin-fin heat sinks," *Energy Sources, Part A: Recovery, Utilization and Environmental Effects*, Vol. 31, No. 1, pp. 51-65, 2009.
- [7] T. J. John, B. Mathew, H. Hegab, "Characteristic Study on the Optimization of Pin-Fin Micro Heat Sink," *2009 AMSE International Mechanical Engineering Congress and Exposition*, Lake Buena Vista, FL, 2009.
- [8] S. Chintada, K.-H. Ko, N.K. Anand, "Heat transfer in 3-D serpentine channels with right-angle turns," *Numerical Heat Transfer; Part A: Applications*, vol. 36, no. 8, pp. 781-806, 1999.
- [9] H. Shaikatullah, W. R. Storr, B. J. Hansen, M. A. Gaynes, "Design and optimization of pin fin heat sinks for low velocity applications," *IEEE transactions on components, packaging, and manufacturing technology. Part A*, vol. 19, no. 4, pp. 486-494, 1996.
- [10] S. Torii, and W.-J. Yang, "Thermal transport phenomena over slot-perforated flat fins with heat sink in forced convection environment," *Proceedings of the ASME Heat Transfer/Fluids Engineering Summer Conference 2004, HT/FED 2004*. pp. 79-84.